ISABE-2015-20060

EFFECT OF REYNOLDS NUMBER ON GROOVE CASING TREATMENT IN A TRANSONIC COMPRESSOR

Qingjun Zhao[1, 3], Xiaoyong Zhou[1, 2], Fei Tang[1], Xiaorong Xiang[1]
1. Institute of Engineering Thermophysics, Chinese Academy of Sciences;
2. University of Chinese Academy of Sciences;
3. Key Laboratory of Light-duty Gas-turbine, Chinese Academy of Sciences
Beisihuan West Road No. 11, Beijing, China, 100190

Abstract

This paper presents a numerical investigation on the effect of Reynolds Number on the Groove Casing Treatment in NASA rotor 67. The results indicate that the blade loading near the casing decreases as the Reynolds number decreases, which weakens the flow exchange between the blade passage and the grooves. Compared with the low Reynolds number case, the positive axial momentum injected into the blade passage from the grooves is higher and the negative axial momentum through the tip gap is reduced more significantly at high Reynolds number. Thus the groove casing treatment is more effective in reducing the low momentum area due to the tip leakage flow and repositioning the interface between the tip leakage flow and incoming flow downstream at high Reynolds number in contrast to low Reynolds number. This results in a higher stall margin improvement at high Reynolds Number than low Reynolds Number. In order to improve the stall margin of the compressor at low Reynolds Number further, two configurations with air injection at the bottom of one groove are tested. The configuration with air injection near the leading edge (CG_1) reduces the blockage due to the tip leakage flow and delays the spillage of the tip leakage flow more effectively by higher injected axial momentum at the front part of the blade. Whereas the configuration with air injection after the shock (CG_4) suppresses the boundary layer separation more effectively by higher injected axial momentum at the rear part of the blade. Consequently, the CG_1 configuration enhances the flow stability of the compressor more effectively than the CG_4 configuration.

Nomenclature

H	momentum flow rate
m	mass flow rate
PR	total pressure ratio
P	total pressure
T	total temperature

Subscripts

s	near stall point
in	inlet
SC	smooth casing
CG	casing grooves
low	low Reynolds Number
cor	converted

Introduction

The aerodynamic instability including rotating stall limits the stable operating range of compressors. The stall of compressors generally starts in the blade tip region. For transonic compressors, complex interaction of the shock, the tip leakage vortex and the boundary layer separation exists near the casing, which can cause flow blockage and have adverse impact on the aerodynamic stability[1-3]. In order to improve the flow field in the blade tip region and increase the stall margin of compressors, numerous casing treatment configurations have been investigated by the researchers[4-6]. In recent years, circumferential groove casing treatments[7, 8] and slot casing treatments[9-10] are most widely

studied. Compared to slot casing treatments, circumferential groove casing treatments usually generate lower stall margin improvement but induce smaller efficiency losses[11].

There have been many investigations that tried to reveal the mechanisms responsible for stall margin improvement caused by circumferential groove casing treatments. Rabe and Hah[12] examined the two-dimensional boundary layer effect, tangential velocity effect, end wall boundary layer effect and leakage vortex segmentation effect which are caused by the casing grooves in a transonic compressor. They identified that the reduction of the incidence near the leading edge of the pressure side is the main mechanism for stall margin improvement owing to the circumferential groove casing treatment. Wilke and Kau[13] numerically investigated the effect of circumferential groove casing treatment on the tip leakage flow in a transonic compressor. The results indicated that casing grooves enhanced the flow stability because the casing grooves could reduce the losses of the tip leakage vortex and prevent the vortex breakdown. Muller et al[14] investigated the circumferential groove casing treatment in a transonic compressor by numerical simulation and experiment. They concluded that two effects were responsible for the stall margin improvement induced by the casing grooves. The first effect was that the blade loading near casing is reduced and thus the velocity of the tip leakage flow is lower. The second effect was that the tip leakage vortex was weakened by the flow into and out of the grooves. Chen et al[15] and Huang et al[16] uncovered the flow mechanisms of the circumferential groove casing treatment in a transonic compressor quantitatively. The mass and momentum transportation carried by the tip leakage flow and the groove flow were analyzed. The positive axial momentum could be injected into the blade passage from the grooves and the negative axial momentum through the tip gap was reduced, so the stall margin of the compressor was improved.

The investigation on casing treatments mainly focused on the high Reynolds number condition. When the aircraft engine is working at the high altitude and low flight Mach number condition, the air density is low and the kinematic viscosity coefficient is large. The performance of the compressor is affected by the low Reynolds number. The boundary layer separation occurs more easily at the low Reynolds number condition compared to the high Reynolds number condition. The blade loading distribution in the blade tip region can be changed when the Reynolds number is reduced, which will affect the intensity of the tip leakage flow. The structure and the intensity of the shock will also change with the decrease of the Reynolds number. Thus, the blade tip flow field at low Reynolds number has different features with that at high Reynolds number[17-19]. Besides, the interaction between the casing grooves and the flow field near the blade tip can be affected by the Reynolds number. The effectiveness of the circumferential groove casing treatment in improving the stall margin at different Reynolds number conditions need to be further explored.

For these reasons, the influence of the Reynolds number on the effectiveness of the circumferential groove casing treatment in a transonic compressor is analyzed. The investigation is implemented with three dimensional numerical simulations.

Investigated compressor and casing grooves

The transonic axial compressor NASA Rotor 67 was used for this investigation. The detail aerodynamic parameters of NASA Rotor 67 can be found in Reference 20-22.

Some overall design parameters are listed in Table 1. Previous studies indicated that the grooves near the leading edge and trailing edge contributed little to the stall margin improvement. And the ratio of the open area to the treated area of the grooves should be kept between 0.65 and 0.75[23]. Based on these results, the casing grooves in this paper are located from 7.5% to 92.5% tip axial chord. The width and depth of the grooves is 10% tip axial chord. And the width of the gap between the grooves is 5% tip axial chord, as shown in Figure 1.

Table 1 Design parameters of NASA Rotor 67

Rotational speed (rpm)	16042.8
Number of rotor blades	22
Design mass flow rate (kg/s)	33.25
Adiabatic efficiency	0.896
Total pressure ratio	1.629
Tip inlet relative Mach number	1.379
Tip clearance/Span	0.71%
Tip speed (m/s)	429

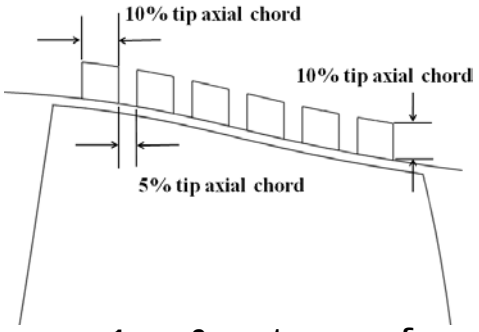

Figure 1 Geometry of the circumferential groove casing treatment

Numerical Method

The commercial CFD software ANSYS CFX was used for the numerical simulation. The steady RANS equations were solved with the two equation SST turbulence model and the Gamma Theta transition model. The Gamma Theta transition model was a correlation-based transition model, which was developed to cover standard bypass transition and flows in low free-stream turbulence environments. Langtry et al[24] validated the Gamma Theta transition model and SST turbulence model for several turbomachinery test cases including a highly loaded compressor cascade, a low pressure turbine blade and a transonic turbine guide vane cascade with CFX software. The numerical method captured the effect of Reynolds Number, the transition location and boundary layer separation well.

The grid topology of the the casing grooves and the blade passage is shown in Figure 2. The blade passage was meshed with HOH topology. The blade passage included 1000000 grid points in total. The blade passage was meshed with 73 grid points in the span-wise direction and 65 grid points in the blade-to-blade direction. The O-grid had 265 grid points in the circumferential direction. The tip clearance was meshed with butterfly topology. There were 17 nodes in the radial direction for the tip clearance. The casing grooves were meshed in H topology. A single groove had 33 grid points in both the axial and the radial direction, and was meshed with 65 grid points in the circumferential direction. The grid density was increased towards the solid boundaries to meet the resolution requirement of y+<2. The blade passage mesh and the grooves mesh were connected with the general grid interface (GGI) method.

The solid boundaries were applied with adiabatic and no-slip boundary conditions. At the inlet boundary, total pressure and total temperature were set. At the outlet boundary, static back pressure was set and radial equilibrium equation was used to obtain the static pressure distribution. The numerical stall was approached by gradually increasing the static back pressure. The last converged working condition with higher back pressure than the

stall point is considered as the near stall point.

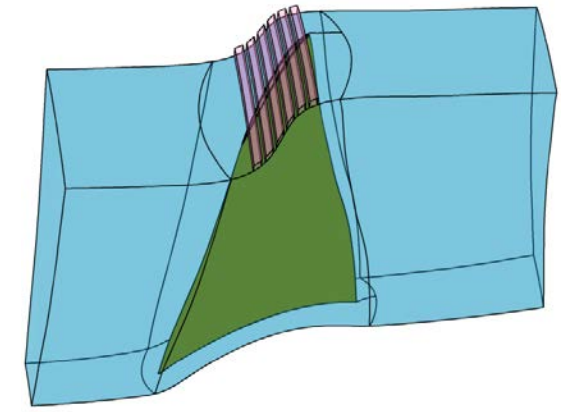

a)

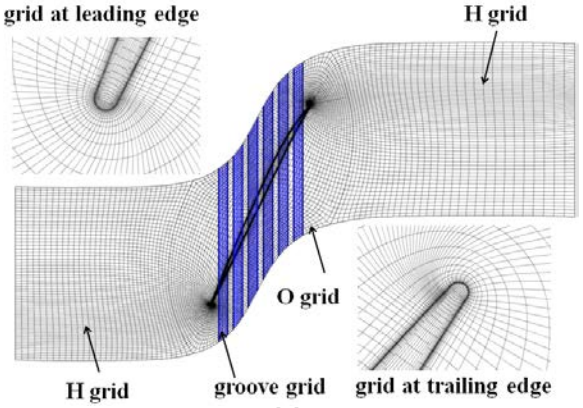

b)

Figure 2 Grid topology of the blade passage and the casing grooves

Validation of the Numerical Method

Figure 3 compares the numerical and experimental overall performance of Rotor 67 with smooth casing. The calculated variation trend of total pressure ratio and adiabatic efficiency with mass flow has good agreement with the experimental result. Meanwhile, there is some difference between the numerical data and the experimental data. The error of total pressure ratio is within 4.5% and error of adiabatic efficiency is within 2.5%. Besides, the normalized near stall mass flow obtained by the calculation is 0.923, and the normalized near stall mass flow obtained by the experiment is 0.921. The numerical simulation can predict the near stall mass flow correctly.

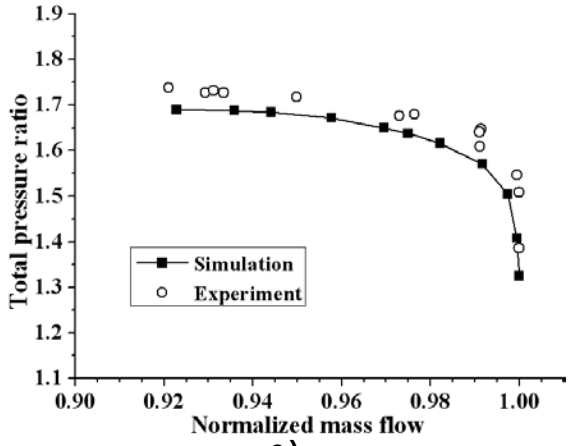

a)

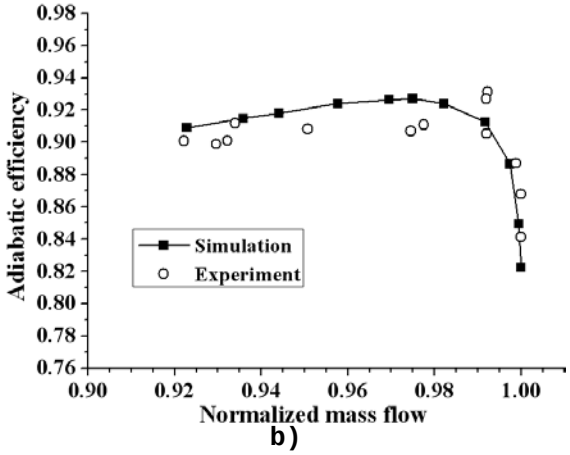

b)

Figure 3 Numerical and experimental overall performance of NASA Rotor 67 at design speed

Figure 4 shows the span-wise distributions of total pressure ratio and total temperature ratio at the near stall condition. The computation can predict the variation trend of total pressure ratio and total temperature ratio along the span-wise direction well. The maximum error of total pressure ratio is within 4.0% and the maximum error of total temperature ratio is within 3.5%. In general, the numerical method is able to predict the performance and the main flow characteristics of the transonic rotor well.

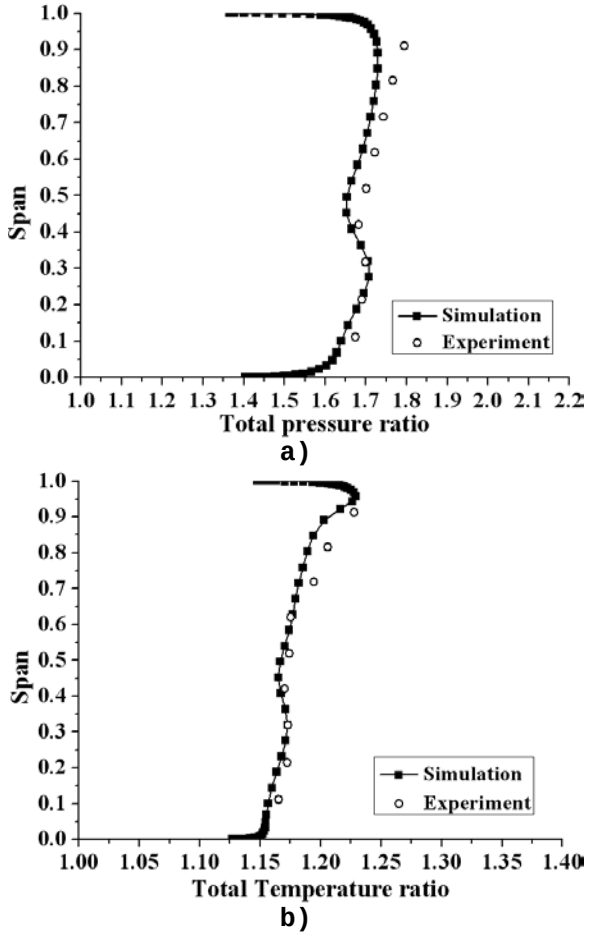

Figure 4 Numerical and experimental span-wise profiles of total pressure ratio and total temperature ratio at the near stall condition

Overall Performance of the Compressor

Two typical Reynolds number conditions are investigated in this paper. They are the ground working condition and the high altitude working condition (20 km, 0.6 Mach number). At the ground working condition, the inlet total pressure is 101325 Pa, the inlet total temperature is 288.15 K and the Reynolds Number is 1.96×10^6. At the high altitude working condition, the inlet total pressure is 7052.26 Pa, the inlet total temperature is 232.25 K and the Reynolds Number is 1.53×10^5.

Figure 5 shows the effect of the circumferential groove casing treatment on the overall performance of the transonic compressor at high and low Reynolds number. In the Figure, SC stands for the case of smooth casing and CG stands for the case of circumferential groove casing treatment. The mass flow of the compressor at low Reynolds number is the converted mass flow, which is calculated by the following equation:

$$m_{cor} = m_{low} \times \frac{101325}{P_{in}} \times \sqrt{\frac{T_{in}}{288.15}} \quad (1)$$

where m_{cor} is the converted mass flow, m_{low} is the actual mass flow at low Reynolds number, P_{in} and T_{in} are inlet total pressure and inlet total temperature at low Reynolds number. The circumferential groove casing treatment has little effect on the efficiency of the compressor. The peak efficiency is improved by 0.12% at high Reynolds number and improved by 0.03% at low Reynolds number with the casing grooves. Meanwhile, the circumferential groove casing treatment increases the stable operating range of the compressor at both high and low Reynolds number. The stall margin improvement (ΔSM) is used to evaluate the effect of the casing grooves on the stability of the compressor. The stall margin improvement is calculated by the following equation:

$$\Delta SM = \left[\frac{(m_s)_{SC}}{(m_s)_{CG}} \cdot \frac{(PR_s)_{CG}}{(PR_s)_{SC}} - 1\right] \times 100\% \quad (2)$$

where $(m_s)_{SC}$ and $(PR_s)_{SC}$ represent mass flow and total pressure ratio at the near stall point of the smooth casing. And $(m_s)_{CG}$ and $(PR_s)_{CG}$ represent mass flow and total pressure ratio at the near stall point of the groove casing treatment. The casing grooves improve the stall margin by 9.40% at high Reynolds number and improve the stall margin by 1.48% at low Reynolds number. The groove casing treatment is more effective in improving the stall margin at the high Reynolds number condition compared to the low Reynolds number condition.

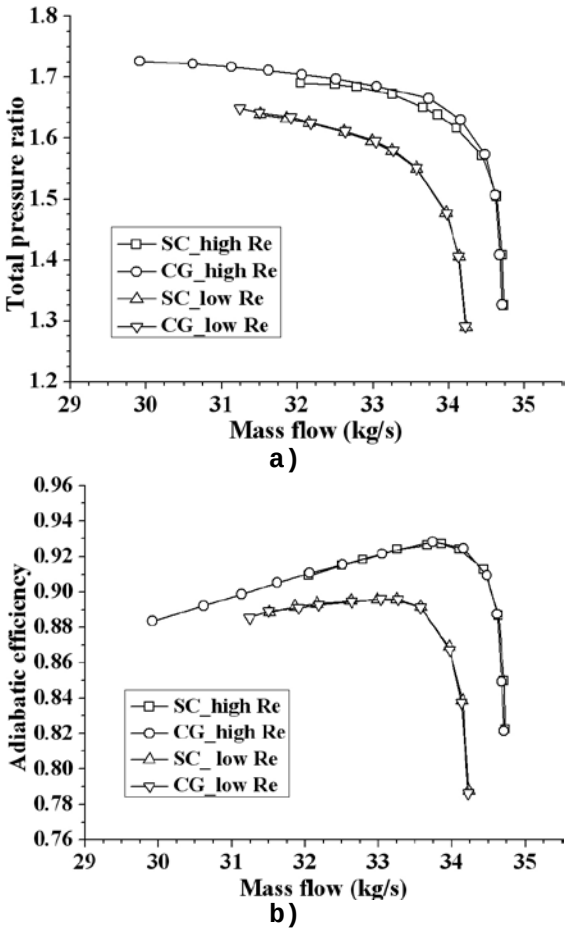

Figure 5 Overall performance of the transonic compressor with and without casing grooves at high and low Reynolds number condition

Analysis of the stall margin improvement due to casing grooves at different Reynolds number conditions

Figure 6 shows the relative Mach number distributions near the blade tip at the near stall mass flow of the smooth casing and at high Reynolds number. In the case of the smooth casing, a large low speed region is formed in the blade passage due to the interaction between the tip leakage vortex and the shock. The low speed region at the blade suction surface caused by the boundary layer separation is small. The flow blockage caused by the tip leakage vortex is mainly responsible for the stall of the compressor. In the case of the groove casing treatment, the low speed region caused by the tip leakage vortex is significantly reduced. The blockage in the blade tip region is alleviated, which results in the improvement of the stall margin. Figure 7 shows the relative Mach distributions near the blade tip at the near stall mass flow of the smooth casing and at low Reynolds number. At the low Reynolds number condition, in addition to the low speed region caused by the tip leakage vortex, there is a large low speed zone near the blade suction surface caused by the boundary layer separation. The tip leakage vortex and the suction surface flow separation are both important factors which are responsible for the blockage near the casing. The low speed regions owing to the tip leakage vortex and the suction side separation are not effectively reduced by the groove casing treatment. It indicates that the groove casing treatment is more effective in reducing the blockage near the blade tip at the high Reynolds number condition compared to the low Reynolds number condition.

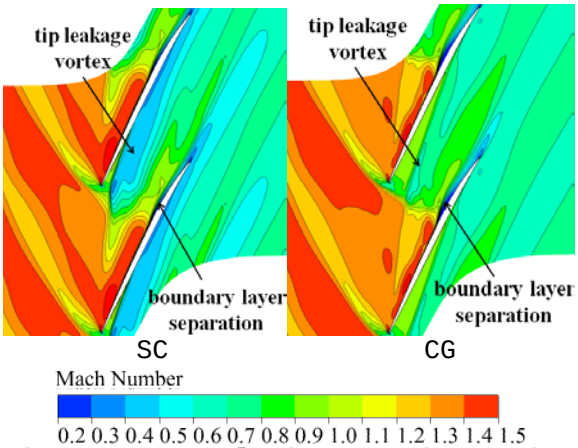

Figure 6 Relative Mach number distributions at the near stall mass flow of the smooth casing and at high Reynolds number (98% span)

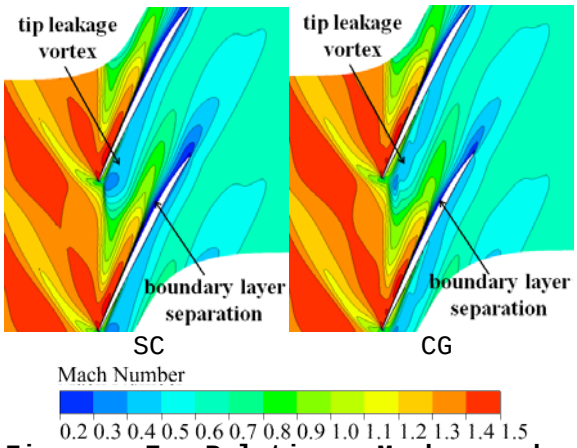

Figure 7 Relative Mach number distributions at the near stall mass flow of the smooth casingand at low Reynolds number (98% span)

Figure 8 shows the entropy distributions near the blade tip at the near stall mass flow of the smooth casing and at high Reynolds number. There is a high entropy region which is caused by the tip leakage flow. The line separating the high entropy region and low entropy region can be considered as the interface between the tip leakage flow and the incoming flow. Vo[25] proposed a criterion of compressor stall. The criterion is that the interface between the tip leakage flow and the incoming flow reaches the leading edge plane and the tip leakage flow spills into the adjacent blade passage. As shown in Figure 4, the interface between the tip leakage flow and the main flow is almost parallel to the leading edge plane at the near stall point of the smooth casing. So the compressor studied in this paper follows the criterion of compressor stall. With the groove casing treatment, the interface between the tip leakage flow and the main flow is further from the leading edge of the pressure side. The leading edge spillage of the tip leakage flow is delayed. Figure 9 shows the entropy distributions near the blade tip at the near stall mass flow of the smooth casing and at low Reynolds number. At the low Reynolds number condition, the groove casing treatment changes the location of the interface of the tip leakage flow and incoming flow little.

Above all, the groove casing treatment is more effective in reducing the blockage near the blade tip and repositioning the interface between the tip leakage flow and incoming flow towards the trailing edge at high Reynolds number compared to low Reynolds number. As a result, the stall margin improvement induced by the casing grooves at high Reynolds number is larger than that at lower Reynolds number.

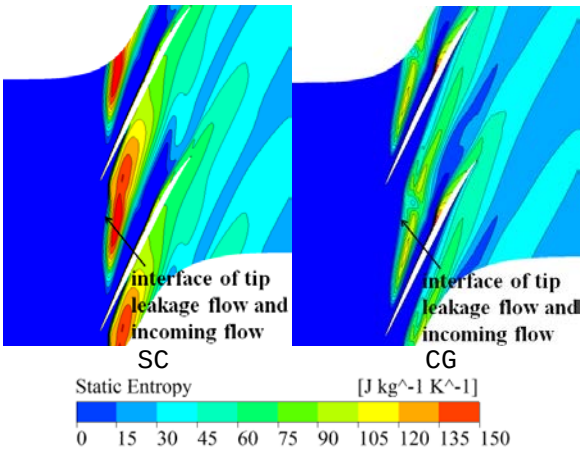

Figure 8 Entropy distributions at the near stall mass flow of the smooth casing and at high Reynolds number (98% span)

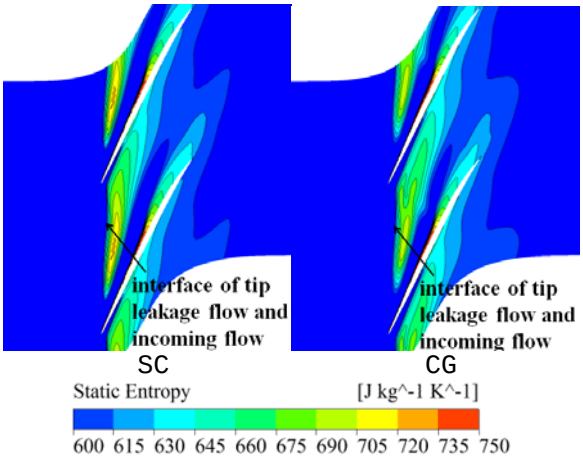

Figure 9 Entropy distributions at the near stall mass flow of the smooth casing and at low Reynolds number (98% span)

Figure 10 shows the normalized flow density distributions at the interface between the casing grooves and the blade passage. The flow density is the product of the density and the normal velocity. The flow density is normalized by the averaged inlet flow density of the compressor. The normal velocity is positive when the fluid in the blade passage enters the grooves, and the normal velocity is negative when the fluid is injected from the the grooves to the blade passage. The high positive flow density region is mainly located near the pressure surface, while the high negative flow density region is mainly located near the suction surface. Namely, the casing grooves can bleed the tip leakage flow into the grooves near the pressure side. Then the grooves transport the bleed fluid in the circumferential direction and inject it into the main flow near the suction surface. This effect reduces the negative axial momentum injected into the blade passage through the tip gap. Figure 11 shows the normalized mass flow rate into the casing grooves (normalized by the compressor inlet mass flow rate and equal to the normalized mass flow rate out of the casing grooves). The normalized mass flow rate into the second groove from the blade passage at low Reynolds number is slightly larger than that at high Reynolds number, whereas the normalized mass flow rate into all the other grooves at low Reynolds number is lower than that at high Reynolds number. Meanwhile, the negative normalized axial momentum flow rate through the tip gap (normalized by the compressor inlet axial momentum flow rate) is reduced from 1.47% to 0.92% at high Reynolds number, while it is reduced from 1.29% to 1.06% at low Reynolds number. This indicates that the groove casing treatment is more effective in reducing the negative axial momentum through the tip gap at high Reynolds number compared to low Reynolds number.

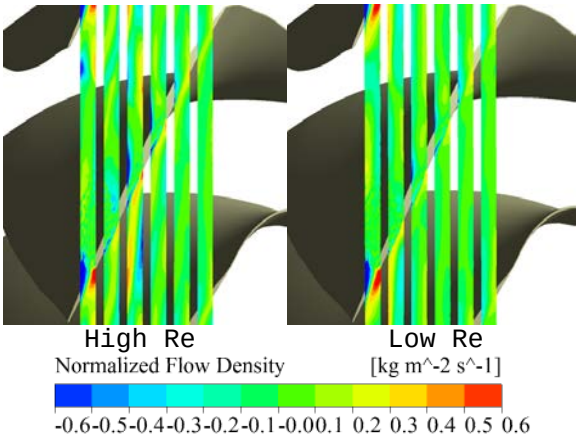

Figure 10 Flow density distributions at the interface of the grooves and the blade passage at the near stall mass flow of the smooth casing

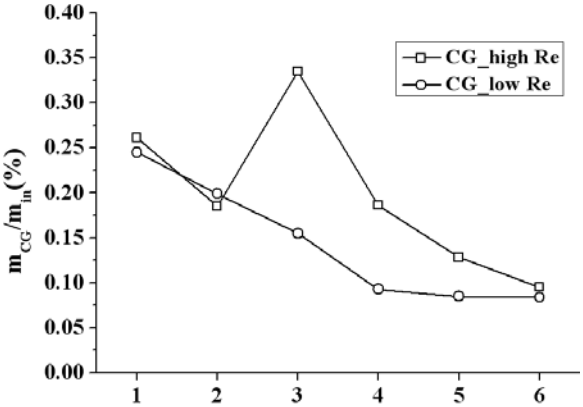

Figure 11 Normalized mass flow rate into the casing grooves at the near stall mass flow of the smooth casing

With smooth casing, the axial momentum can only be injected into the blade passage through the tip gap. But with the groove casing treatment, the axial momentum can also be injected into the blade passage through the interface between the grooves and the blade passage. Figure 12 shows the net normalized axial momentum flow rate injected into the blade passage from the casing grooves (normalized by the compressor inlet axial momentum flow rate). Except for the last groove, the positive axial momentum flow rate injected into the blade passage from all the other grooves at high Reynolds number is larger than that at low Reynolds number.

Overall, compared with the low Reynolds number condition, the the negative axial momentum through the tip gap is reduced more effectively and the positive axial momentum injected into the blade passage from the grooves is larger at high Reynolds number condition. Thus, the groove casing treatment is more effective in reducing the blockage caused by the tip leakage flow and delaying the leading edge spillage of the tip leakage flow at high Reynolds number compared to low Reynolds number. Meanwhile, because the axial momentum injected into the blade passage from the grooves at the rear part of the blade is little, the boundary layer separation cannot be effectively suppressed at low Reynolds number.

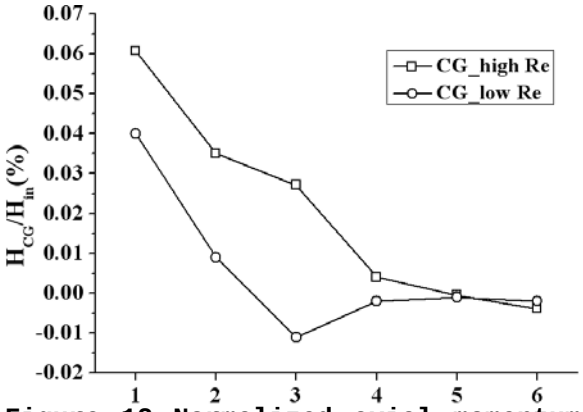

Figure 12 Normalized axial momentum flow rate into the blade passage at the near stall mass flow of the smooth casing

Figure 13 shows the static pressure coefficient distributions at 99% span. The axial extent of the grooves is also shown in the Figure. The static pressure coefficient is equal to static pressure divided by the inlet total pressure of the compressor. The groove casing treatment changes the blade loading distribution near the blade tip. This changes the driving force of the tip leakage flow. The groove near the leading edge reduces the pressure difference over the blade tip significantly, which is beneficial to reduce the intensity of the tip leakage flow. Besides, the driving force for the flow into and out of grooves is the pressure difference between the pressure side and the suction side near the tip. With the decrease of the Reynolds number, the boundary layer separation region at the suction side is increased and the intensity of the shock is decreased, thus the blade loading near the casing is reduced. As a result, the intensity of the mass and momentum exchange between the blade passage and the grooves at low Reynolds number is lower than that at high Reynolds number.

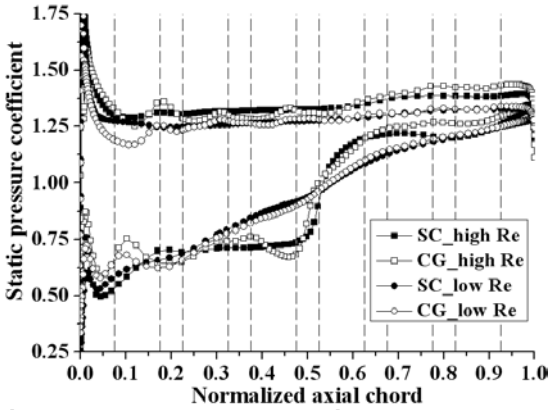

Figure 13 Static pressure coefficient distributions at the near stall mass flow of the smooth casing (99% span)

<u>Analysis of the stall margin improvement due to the casing grooves with injection at the bottom at low Reynolds number condition.</u>

In order to improve the stall margin of the compressor at the low Reynolds number condition more effectively, two modified casing treatment configurations with air injection at the bottom of one groove are tested. The geometry of the casing grooves is not changed. One configuration is injecting air at the bottom of the first groove from the leading edge (CG_1), and the other configuration is injecting air at the bottom of the fourth groove from the leading edge (CG_4). The injection mass flow is equal to 1% near stall mass flow of the smooth casing at low Reynolds number.

The injection velocity is normal to the bottom of the groove. And the injection total temperature is equal to the inlet total temperature of the compressor. The configuration with air injection at the bottom of the first groove obtains a stall margin improvement of 4.07%. And the configuration with air injection at the bottom of the fourth groove obtains a stall margin improvement of 3.00%.

Figure 14 shows the relative Mach number distributions near the blade tip at the near stall mass flow of the smooth casing. The location of the groove with air injection at the bottom is also shown in the figure. The CG_1 configuration is more effective in reducing the low speed region caused by the tip leakage vortex near the leading edge of the pressure side than the CG_4 configuration, while the CG_4 configuration is more effective in reducing the low speed region induced by the boundary layer separation than the CG_1 configuration.

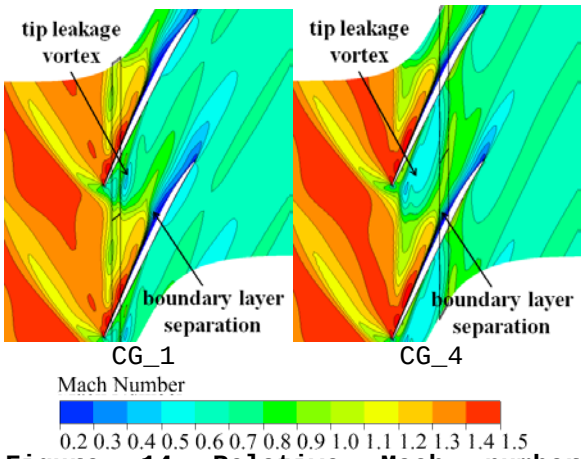

Figure 14 Relative Mach number distributions at the near stall mass flow of the smooth casing and at low Reynolds number (98% span)

Figure 15 shows the entropy distributions near the blade tip for the CG_1 and CG_4 configuration at the near stall mass flow of the smooth casing. With the CG_4 configuration, the interface between the tip leakage flow and the incoming flow changes little compared to the configuration without injection. However, with the CG_1 configuration, the interface between the tip leakage flow and the incoming flow is further from the leading edge of the pressure side. The spillage of the tip leakage flow near the leading edge can be suppressed.

Overall, The CG_1 configuration is more effective in reducing the blockage due to the tip leakage flow near the leading edge of the pressure side and delaying the leading edge spillage of the tip leakage flow, while the CG_4 configuration is more effective in reducing the low speed region due to the boundary layer separation. With the CG_4 configuration, there is still a large low speed region caused by the tip leakage vortex near the leading edge of the pressure side which can blocks the incoming flow. Besides, the leading edge spillage of the tip leakage flow cannot be delayed effectively. Consequently, the CG_1 configuration improves the stall margin of the compressor more effectively than the CG_4 configuration.

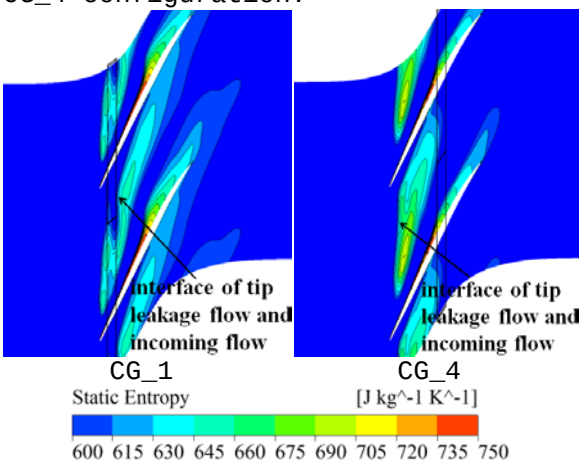

Figure 15 Entropy distributions at low Reynolds number and at the near stall mass flow of the smooth casing (98% span)

Figure 16 shows the net normalized axial momentum flow rate injected into the blade passage from

the casing grooves for the CG_1 case, the CG_4 case and the case without injection. Compared to the configuration without air injection, the CG_1 configuration increases the axial momentum injected into the blade passage from the first two grooves obviously. But the CG_1 configuration changes the axial momentum injected into the blade passage from the last four grooves little. Thus, the CG_1 configuration is more effective in energizing the low momentum fluid from the tip leakage flow near the leading edge and suppressing the leading edge spillage of the tip leakage flow. For the CG_4 configuration, the axial momentum injected into the blade passage from the first two grooves decreases. But the axial momentum injected into the blade passage from the last three grooves increases significantly. So the CG_4 configuration is more effective in energizing the low speed fluid due to the boundary layer separation at the rear part of the blade.

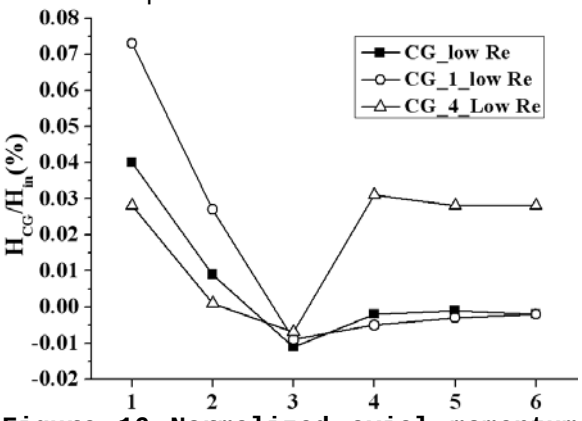

Figure 16 Normalized axial momentum flow rate into the blade passage at the near stall mass flow of the smooth casing

Injecting air at the bottom of the casing grooves also changes the blade loading near the tip. As shown in Figure 17, the CG_1 configuration increases the static pressure near the leading edge of the pressure side. The CG_4 configuration increases the static pressure near the pressure side along the entire axial chord. The driving force for the tip leakage flow is strengthened, and this will have negative effect on the flow stability. Meanwhile, the tip leakage flow can be weakened by the flow into and out of the grooves. With the combined effect of these factors, the negative normalized axial momentum flow rate through the tip gap is 1.05% for the CG_1 configuration and 1.06% for the CG_2 configuration. They are almost identical to the normalized axial momentum flow rate through the tip gap for the configuration without injection. The modified configurations have little effect on the negative axial momentum through the tip gap.

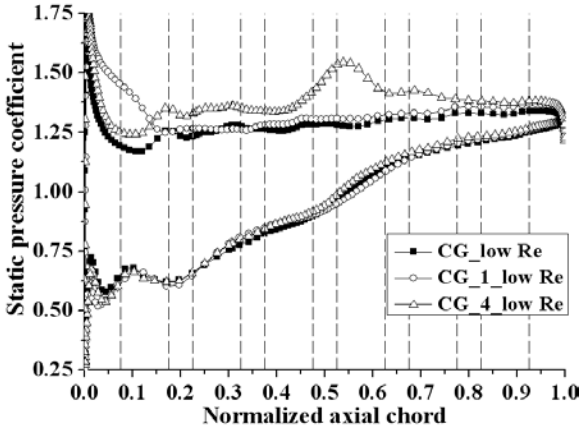

Figure 17 Static pressure coefficient distributions at the near stall mass flow of the smooth casing (99% span)

Conclusions

A numerical investigation on the circumferential groove casing treatment in NASA rotor 67 at two different Reynolds numbers is conducted in this paper. The conclusions are summarized as follows:

(1) As the Reynolds number is reduced, the flow separation zone at the suction side is enlarged and the intensity of the shock is reduced, which decreases the blade loading near the blade. Hence, the intensity of the mass and momentum exchange between the blade passage and the

grooves is reduced. The positive axial momentum injected into the blade passage from the grooves becomes lower and the negative axial momentum through the tip gap is reduced less effectively. Therefore, at low Reynolds Number, the casing grooves have little effect on the location of the interface between the tip leakage flow and incoming flow. And the low speed regions caused by the tip leakage vortex and boundary layer separation are not reduced effectively. Whereas at high Reynolds Number, the casing grooves reduce the blockage from the tip leakage vortex and delay the leading edge spillage of the tip leakage flow significantly. So the groove casing treatment obtains a larger stall margin improvement at high Reynolds number compared to low Reynolds number.

(2) At low Reynolds number, two modified configurations with air injection at the bottom of one of the grooves are investigated. The configuration with air injection near the leading edge (CG_1) increases the axial momentum injected from the grooves to the blade passage in the front part of of the blade, while the configuration with air injection after the shock (CG_4) increases the axial momentum injected from the grooves to the blade passage in the rear part of of the blade. As a result, the CG_1 configuration is more effective in energizing the low speed fluid from the tip leakage flow near the leading edge and delaying the leading edge spillage of the tip leakage flow, while the CG_4 configuration is more effective in alleviating the boundary layer separation. As a result, the CG_1 configuration is more effective in improving the stall margin than the CG_4 configuration.

Acknowledgments

This work has been carried out with the support of National Basic Research Program of China (No. 2010CB227302) and National Natural Science Foundation of China (No. 51206162). The authors would like to thank them for funding it and their permission to publish this paper.

References

[1] Yamada K, Funazaki K, Furukawa M. The Behavior of Tip Clearance Flow at Near-Stall Condition in a Transonic Axial Compressor Rotor[C]. ASME Turbo Expo 2007: Power for Land, Sea, and Air, Montreal, Canada, May 14-17, 2007, Paper GT 2007-27725.

[2] Biollo R, Benini E. Shock/Boundary-Layer/Tip Clearance Interaction in a Transonic Rotor Blade[J]. Journal of Propulsion and Power, 2009, 25(3): 668-677.

[3] Pengfei Ju, Fangfei Ning. Numerical Investigation of the Prestall Behavior in a Transonic Axial Fan Rotor[C]. ASME Turbo Expo 2014: Turbine Technical Conference and Exposition, Dusseldorf, Germany, June 16-20, 2014, Paper GT2014-25502.

[4] Hathaway M D. Passive Endwall Treatments for Enhancing Stability[R]. NASA TM-214409, 2007.

[5] Pixberg C T, Schiffer H-P, Ross M H, et al. Stall Margin Improvement by Use of Casing Treatment[C]. ASME Turbo Expo 2013: Power for Land, Sea, and Air, San Antonio, Texas, USA, June 3-7, 2013, Paper GT2013-95842.

[6] Alone D B, Kumar S S, Thimmaiah S. Experimental Investigation on the Effect of Porosity of Bend Skewed Casing Treatment on a Single Stage Transonic Axial Flow Compressor[C]. ASME Turbo Expo 2014: Turbine Technical Conference and Exposition, Dusseldorf, Germany, June 16-20, 2014, Paper GT2014-26102.

[7] Hah C. Toward Optimum Configuration of Circumferential Groove Casing Treatment in Transonic Compressor Rotors[C]. ASME-JSME-KSME Joint Fluids

Engineering Conference, Hamamatsu, Japan, July 24-29, 2011, Paper AJK2011-05020.
[8] Sakuma Y, Watanabe T, Himeno T, et al. Numerical Analysis of Flow in a Transonic Compressor with a Single Circumferential Casing Groove: Application to Two Different Compressor Rotors[C]. ASME Turbo Expo 2014: Turbine Technical Conference and Exposition, Dusseldorf, Germany, June 16-20, 2014, Paper GT2014-26691.
[9] Legras G, Castillon L, Trebinjac I. Flow Mechanisms induced by Non-Axisymmetric Casing Treatment in a Transonic Axial Compressor[C]. Proceedings of the 10th International Symposium on Experimental Computational Aerothermodynamics of Internal Flows, Brussels, Belgium, 4-7 July, 2011, ISAIF10-158.
[10] Schonweitz D, Voges M, Gonis G, et al. Experimental and Numerical Examinations of a Transonic Compressor-Stage with Casing Treatment[C]. ASME Turbo Expo 2013: Power for Land, Sea, and Air, San Antonio, Texas, USA, June 3-7, 2013, Paper GT2013-95550.
[11] Muller M W, Kau H-P, Voges M, et al. Investigation of Passage Flow Features in a Transonic Compressor Rotor with Casing Treatments[C]. ASME Turbo Expo 2011: Turbine Technical Conference and Exposition, Vancouver, British Columbia, Canada, June 6-10, 2011, Paper GT2011-45404.
[12] Rabe D C, Hah C. Application of Casing Circumferential Grooves for Improved Stall Margin in a Transonic Axial Compressor[C]. ASME Turbo Expo 2002: Power for Land, Sea, and Air, Amsterdam, the Netherlands, June 3-6, 2002, Paper GT2002-30641.
[13] Wilke I, Kau H -P. A Numerical Investigation of the Influence of Casing Treatments on the Tip Leakage Flow in a HPC Front Stage[C]. ASME Turbo Expo 2002: Power for Land, Sea, and Air, Amsterdam, the Netherlands, June 3-6, 2002, Paper GT2002-30642.
[14] Muller M W, Schiffer H-P, Hah C. Effect of Circumferential Grooves on the Aerodynamic Performance of an Axial Single-Stage Transonic Compressor[C]. ASME Turbo Expo 2007: Power for Land, Sea, and Air, Montreal, Canada, May 14-17, 2007, Paper GT2007-27365.
[15] Chen Haixin, Huang Xudong, Shi Ke, et al. A CFD Study of Circumferential Groove Casing Treatments in a Transonic Axial Compressor[C]. ASME Turbo Expo 2010: Power for Land, Sea, and Air, Glasgow, UK, June 14-18, 2010, Paper GT2010-23606.
[16] Huang Xudong, Chen Haixin, Shi Ke, et al. An Analysis of the Circumferential Grooves Casing Treatment for Transonic Compressor Flow[J]. Science China (Physics, Mechanics & Astronomy), 2010, 53(2): 353-359.
[17] Hah C, Enomoto S J, Hobson G V. Numerical and Expermiental Investigation of Low Reynolds Number Effects on Laminar Flow Separation and Transition in a Cascade of Compressor Blade[C]. ASME Turbo Expo 2000, Munich, Germany, May 8 -11, 2000, Paper 2000-GT-276.
[18] Min Zhou, Rugen Wang, Yun Bai, et al. Research on Flow Instability Triggering Process at Stall Condition of Transonic Compressor Rotor at Low Reynolds Number[J]. Journal of Aerospace Power, 2009, 24(6): 1378-1384.
[19] Hui Du, Shengfeng Zhao, Jianbo Gong, et al. Effects of Low Reynolds Number on Flow Stability of a Transonic Compressor[C]. ASME Turbo Expo 2012: Turbine Technical Conference and Exposition, Copenhagen, Denmark, June 11-15, 2012, Paper GT2012-68273.
[20] Walter S C, William S, Donald C U. Design and Performance of a 427-Meter-Per-Second-Tip-Speed Two-Stage Fan Having a 2.40

Pressure Ratio[R]. NASA Technical Paper 1314, 1978.
[21] Strazisar A J, Wood J R, Hathaway, M D, et al. Laser Anemometer Measurements in a Transonic Axial-Flow Fan Rotor[R]. NASA Technical Paper 2879, 1989.
[22] Adamczyk J J, Celestina M L, Greitzer E M. 1993, The Role of Tip Clearance in High-Speed Fan Stall[J]. ASME Journal of Turbomachinery, 1993, 115(1): 28-39.
[23] Evorott E. and Bailoy D. Effects of Grooved Casing Treatment on the Flow Range Capability of a Single Stage Axial-Flow Compressor[R]. NASA TMX-2459, 1972.
[24] Langtry R B, Menter F R, Likki S R, et al. A Correlation-based Transition Model Using Local Variables Part II-Test Cases and Industry Applications[C]. ASME Turbo Expo 2004: Power for Land, Sea, and Air, Vienna, Austria, June 14-17, 2004, Paper GT2004-53454.
[25] Vo H D, Tan C S, Greitzer E M, Criteria for Spike Initiated Rotating Stall[C]. ASME Turbo Expo 2005: Power for Land, Sea, and Air, Reno, Nevada, USA, June 6-9, 2005, Paper GT2005-47306, 2005.